Volume 38 http://acousticalsociety.org/

2019 International Congress on Ultrasonics

Bruges, Belgium

3-6 September 2019

Biomedical Acoustics: MCT+MEI (1/3) Presentation 3

Magnetic force induced vibration of a ferromagnetic sphere for viscoelastic media characterization

Alejandro Cebrecos, Miguel Company, Noé Jiménez, José María Benlloch and Francisco Camarena

Instituto de Instrumentación para Imagen Molecular (i3M) CSIC, Universidad Politécnica de Valencia, Valencia, 46020, SPAIN; alcebrui@epsg.upv.es; micomar3@upvnet.upv.es; nojigon@epsg.upv.es; benlloch@i3m.upv.es; fracafe@fis.upv.es

A new method that combines transient magnetic forces with ultrasonic imaging and allows local experimental characterization of the complex shear modulus of a viscoelastic medium is presented. By measuring the dynamics of a ferromagnetic inclusion under the application of a magnetic force, the viscoelastic properties of the medium are extracted. The system is composed of a coil, which creates a magnetic field that induces displacement on a ferromagnetic particle located inside a test phantom, and an ultrasound transducer operating in pulsed-echo mode, utilized to track the displacement of the particle with spatial resolution of several μm. Experiments were conducted embedding a ferromagnetic sphere on test phantoms with different compositions and at different temperatures. The obtained results are in good agreement with the theoretical estimation of the dynamical response of a sphere and show robustness on the estimation of the viscoelastic parameters.

Published by the Acoustical Society of America

 https://doi.org/10.1121/2.0001200

I. Introduction

Evaluation of the mechanical properties of viscoelastic media is relevant in different areas of research. In medicine, for instance, it has been demonstrated that biomechanical properties of tissue are often correlated with their physiological state [1-3]. The dynamics of a solid sphere under the application of an external force to estimate the viscoelastic properties of the surrounding medium was first studied theoretically by Oestreicher, who employed a Kelvin-Voigt rheological model in a medium with equal stiffness and viscosity[4]. Ilinski investigated the static and transient displacement responses of a sphere and a bubble embedded in an elastic medium[5], and Aglyamov extended the work to viscoelastic media[6]. Finally, Urban proposed a theory to describe a generalized embedded sphere response both in time and frequency domains applicable to any viscoelastic rheological model[7]. Subsequent experimental studies pursued the local characterization of tissue-like phantoms by exciting an embedded sphere making use of the acoustic radiation force (ARF). Greenleaf estimated the viscoelastic properties of gelatin materials at different frequencies[8]. Emelyanov locally assessed the shear modulus of a medium employing the ARF generated at the focus using a short pulse[9]. In this work we propose a method to estimate the viscoelastic parameters of soft-solids. We use a Magneto-motive Ultrasound (MMUS) experimental setup[10], applying an external magnetic force on a macroscopic sphere embedded in a gelatin phantom and tracking its displacement. The experimental setup and a theoretical approximation of the dynamics of the sphere are depicted in Fig. 1. The process encompass an electrical pulse excitation of a coil, which produces an attracting force on the ferromagnetic sphere, a fast sequence of pulse-echo ultrasound signals to accurately track the position of the sphere, and a cross-correlation method to obtain the time-varying displacement of the sphere, from which the elastic parameters of the surrounding medium are obtained employing minimization techniques between the experimental data and the theory.

II. Methodology

II.1 Dynamics of a solid sphere in viscoelastic media

Starting from the equations of motion for a Kelvin-Voigt medium in the frequency domain[6], and considering a rigid sphere embedded in a viscoelastic medium and submitted to a transient external force $F_z^{ext}(t)$, applied on its surface and acting along the z component of the displacement of the sphere, $U_z(\omega)$, the Fourier transforms of the external force $F_z^{ext}(\omega)$ and the displacement are linearly related by[6]

$$F_z^{ext}(\omega) = \left[-M\omega^2 + 6\pi GR\left(1 - ikR - \frac{1}{9}k^2R^2\right)\right]U_z(\omega) \tag{1}$$

Where $M = 4\pi\rho_s R^3/3$ is the mass, ρ_s is the density, R is the radius of the sphere, $G = \mu - i\omega\eta$ is the complex shear modulus, μ and η are the shear elastic and shear viscous coefficients, and k is the complex wave number in the viscoelastic medium given by the dispersion relation $k^2 = \rho\omega^2/(\mu - i\omega\eta)$. In our study, the sphere is subjected to a pulsed magnetic force, assuming an ideal rectangular pulse, with t_0 the duration and F_0 the amplitude of the pulse, as shown in Fig. 1(c). Considering its Fourier transform, $F_z^{ext}(\omega) = -iF_0(e^{i\omega t_0} - 1)/\omega$, combining this expression with Eq. (1) and applying the inverse Fourier transform, the displacement of the solid sphere in a viscoelastic medium is[6]

$$u_z(t) = -\frac{iF_0}{12\pi^2 R}\int_{-\infty}^{\infty}\frac{\left(e^{i\omega t_0} - 1\right)e^{i\omega t}}{\omega(\mu - i\omega\eta)\left(1 - ikR - \frac{k^2R^2(1+2\beta)}{9}\right)}d\omega \tag{2}$$

where $\beta = \rho_s/\rho$ is the normalized density of the sphere with respect to the medium density.

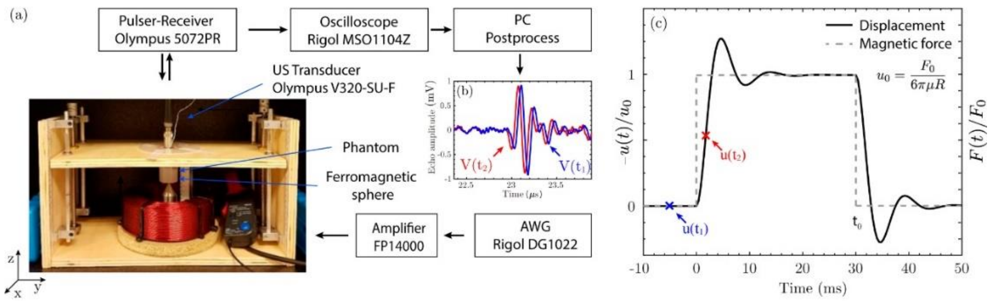

Figure 1.(a) Experimental setup. (b) Example of ultrasonic pulse-echo signals when the sphere is at rest (blue) or in motion (red). (c) Magnetic force waveform of an ideal square pulse (dashed line) and the expected displacement waveform of the sphere in a viscoelastic medium (continuous line)

II.2 Magnetic force exerted on the sphere

The magnetic force $\mathbf{F}$ acting on a small ellipsoid due to the presence of the magnetic flux density B_0 along the z axis can be reduced, if a sphere is considered, to[11]

$$F_z^{\text{ext}}(z,t) = -\frac{4\pi R^3}{\mu_0} B_z(z,t)\frac{\partial B_z(z,t)}{\partial z} \tag{4}$$

Note that for a soft-ferromagnetic sphere the ratio the magnetic field strength, $\mathbf{H}$, and the magnetization of the material, M, do not depend on the magnetic properties of the material[12] and is given by $\mathbf{H} = -3\mathrm{M}$.

II.3 Experimental methods

The experimental setup used in this work is shown in Fig. 1(a). It encompasses a copper coil and a ferritic steel core (AISI 430 steel). The coil is properly excited to produce a roughly square pulse of electrical current of $t_0 = 30$ ms. A Hall magnetometer is used to characterize the magnetic field of the system at steady current. A weighing scale is used to experimentally measure the magnetic force exerted on a ferromagnetic sphere in the absence of the viscoelastic medium. The displacement of the sphere is estimated from the temporal shifts of the pulse-echo signals produced using an A-scan system (see Figs. 1(b, c)). A 7.5 MHz transducer (V320-SU-F, Olympus) is excited with a pulser-receiver (5072PR, Olympus) working at a pulse repetition rate of 2.5 kHz. The position of the sphere on time is given by the cross-correlation between the RF signals and a reference signal acquired when the sphere is at rest[13]. The resolution of the estimated displacement is of 0.3 μm. Two different gelatin phantoms of cylindrical shape and a volume of 25 ml are considered. “Phantom A” is composed of water and gelatin powder with a gelatin concentration of 60 ml/l, while “Phantom B” is composed of water, glycerol and gelatin powder with the same concentration and a glycerol concentration of 40% of the total volume. A 2 mm diameter ferromagnetic sphere (AISI 52100) was introduced during the production of both gelatins at around 15 mm of the bottom surface.

III. Results and discussion

III.1 Magnetic force characterization

We start showing validation of the magnetic forces acting on the sphere in the absence of viscoelastic medium. First, the FEM simulated magnetic field with no sphere is shown in Fig. 2 (a). Then, a direct measurement of the magnetic field of the system around the area where the sphere is placed was performed in static regime, sending a continuous current of 20 A to the coil. The value of the z component of the field was measured along 3 horizontal 40 mm lines, in x direction, at 10 mm, 15 mm and 20 mm distance from the tip of the core, with a good agreement between numerical and experimental results, as shown in Fig. 2 (b). Finally, the magnetic force as a function of distance to the core is shown in Fig. 2 (c), comparing a direct measurement using a weighing scale, an indirect measurement applying Eq. (3) with a 2 mm radius sphere and the experimentally measured magnetic field measured from 3.4 mm from the tip of the core to 23.4 mm, and a FEM simulation including the sphere in the domain, all three showing an excellent agreement. For small displacements around 100 μm and at 20 mm from the tip of the core, force variations are very small with respect to its value, (< 1 %), which justifies our assumption of a constant magnetic force exerted on the moving sphere.

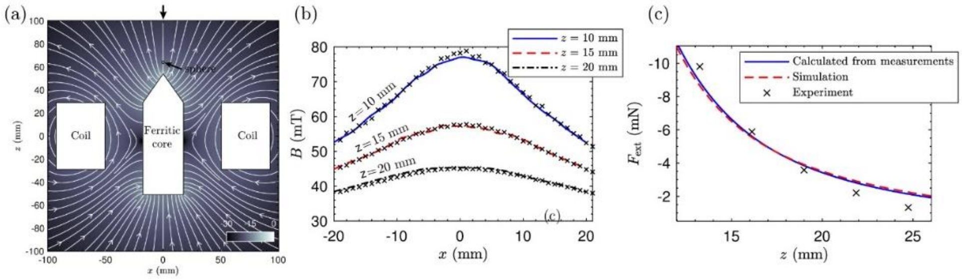

Figure 2. (a) FEM simulated magnetic flux density. (b) Experimental (markers), simulated (continuous) magnetic flux density at different heights. (c) Magnetic force on the sphere measured using a weighing scale (markers), calculated from the measured field (continuous), and simulated (dashed).

III.2 Estimation of viscoelastic parameters

The displacement waveforms corresponding to phantoms A and B are shown in Fig. 3, feeding the coil with pulses of 30 A and 30 ms. The viscoelastic parameters are obtained by minimization techniques comparing the experimental and theoretical displacement waveforms (see Eq. (2)). For phantom A at 24 ºC, the theoretical curve fits the experiments for the first 5-7 ms, as shown in Fig. 3 (a). The initial slope and the amplitude of the first oscillation is fitted by both models, the elastic ($\eta = 0$ Pa $\cdot$ s) and viscoelastic ($\eta \approx 3.961 \times 10^{-14}$ Pa $\cdot$ s), showing the characteristic quasi-elastic behaviour without glycerin at high temperature. In contrast, at low temperature (19 ºC) or when glycerin is introduced in the phantom, the purely-elastic model cannot accurately describe the dynamics of the sphere, as shown in Figs. 3 (b, c), respectively. In these cases, the elastic model overestimates the amplitude of the first oscillation, which is damped proportionally to the viscous modulus. On the contrary, the viscoelastic model correctly fits the experimental data for both viscoelastic phantoms. The experiment was repeated 5 times and the results are listed in Table 1, showing a fairly low variation and hence a good repeatability.

Table 1. Viscoelastic parameters estimated from experiments

	Shear elastic modulus μ (Pa)	Shear viscous modulus η (Pa $\cdot$ s)
Phantom A (24.0 ºC)	650 ± 90	$4 \times 10^{-14} \pm 4 \times 10^{-14}$
Phantom A (19.0 ºC)	1870 ± 90	0.60 ± 0.07
Phantom B (19.3 ºC)	3200 ± 300	1.0 ± 0.1

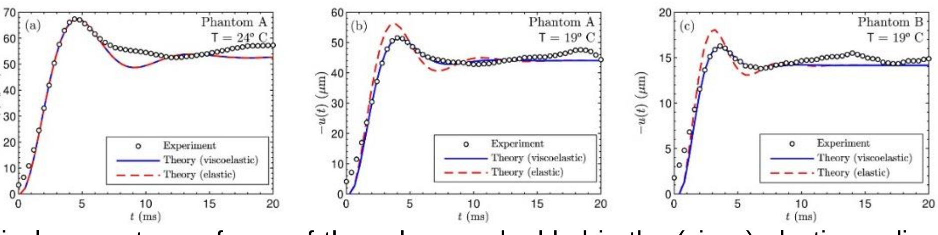

Figure 3. Displacement waveforms of the sphere embedded in the (visco)-elastic media. Phantom A (elastic) measured at (a) T $= 24.0$ ºC and (b) $T = 19.0$ ºC. (c) Phantom B (viscoelastic) at $T = 19.3$ ºC

IV. Conclusion

A new method to characterize the complex shear modulus of viscoelastic media combining magnetic force and ultrasound is presented in this work. The media properties are obtained by measuring the dynamics of a ferromagnetic inclusion. In particular, a coil is used to produce a magnetic force on a ferromagnetic sphere, whose magnetic field was estimated numerically and experimentally. Both the measured magnetic field and forces acting on the sphere agree well with simulations and theory. Finally, the measured displacement of the sphere inside the phantom allows the estimation of the viscoelastic parameters of the surrounding medium.

Acknowledgements
This work is funded by the Spanish Ministerio de Economía e Innovación (MINECO) Generalitat Valenciana (GVA) through the projects TEC2016-80976-R and AICO2016-108. N.J. and A. C acknowledge the support of GVA through the contracts APOSTD/2017/042 and APOSTD/2018/A/229.

References
[1] S. Aglyamov, A. Skovoroda, *Mechanical properties of soft biological tissues, Biophysics*, vol. 45, no. 6 **2000**, 1103–1111.
[2] J. Ophir, S. K. Alam, B. S. Garra, F. Kallel, E. E. Konofagou, T. Krouskop, C. R. Merritt, R. Righetti, R. Souchon, S. Srinivasan, *Elastography: imaging the elastic properties of soft tissues with ultrasound, J. MED ULTRASON*, vol. 29, no. 4 **2002**, p. 155.
[3] A. Sarvazyan, *Elastic properties of soft tissues, NY: Academic Press*, vol. 3 **2001**, pp. 107–127.
[4] H. Oestreicher, *Field and impedance of an oscillating sphere in a viscoelastic medium with an application to biophysics, J. Acoust. Soc. Am*, vol. 23, no. 6 **1951**, pp. 707–714.
[5] Y. Ilinskii, G. Meegan, E. Zabolotskaya, S. Emelianov, *Gas bubble and solid sphere motion in elastic media in response to acoustic radiation force, J. Acoust. Soc. Am*, vol. 117, no. 4 **2005**, pp. 2338–2346.
[6] S. Aglyamov, A. Karpiouk, Y. Ilinskii, E. Zabolotskaya, and S. Emelianov, *Motion of a solid sphere in a viscoelastic medium in response to applied acoustic radiation force: Theoretical analysis and experimental verification, J. Acoust. Soc. Am*, vol. 122, no. 4 **2007**, pp. 1927–1936.
[7] M. W. Urban, I. Z. Nenadic, S. A. Mitchell, S. Chen, and J. F. Greenleaf, *Generalized response of a sphere embedded in a viscoelastic medium excited by an ultrasonic radiation force, J. Acoust. Soc. Am*, vol. 130, no. 3 **2011**, pp. 1133–1141.
[8] S. Chen, M. Fatemi, and J. F. Greenleaf, *Remote measurement of material properties from radiation force induced vibration of an embedded sphere, J. Acoust. Soc. Am*, vol. 112, no. 3 **2002**, pp. 884–889.
[9] A. B. Karpiouk, S. R. Aglyamov, Y. A. Ilinskii, E. A. Zabolotskaya, and S. Y. Emelianov, *Assessment of shear modulus of tissue using ultrasound radiation force acting on a spherical acoustic inhomogeneity, IEEE Trans Ultrason Ferroelectr Freq Control*, vol. 56, no. 11, **2009**.
[10] J. Oh, M. D. Feldman, J. Kim, C. Condit, S. Emelianov, T. E. Milner, *Detection of magnetic nanoparticles in tissue using magnetomotive ultrasound, Nanotechnology*, vol. 17, no. 16 **2006**, p. 4183.
[11] J. Schenck, *Safety of strong, static magnetic fields, J Magn Reson Imaging*, vol. 12, **2000**, 2–19.
[12] R. Fitzpatrick, *Classical electromagnetism, Ed. Createspace Independent Pub*, **2016**.
[13] M. A. Lubinsky, S. Y. Emelianov, M. O'Donnell, *Frequency-and phase-sensitive magnetomotive ultrasound imaging of superparamagnetic iron oxide nanoparticles, IEEE Trans Ultrason Ferroelectr Freq Control*, vol. 46, no. 1 **1999**, pp. 82–96.